WIVERN: a new satellite concept to provide global in-cloud winds, precipitation and cloud properties.

Illingworth, A. J.; Battaglia, A.; Bradford, J.; Forsythe, M.; Joe, P.; Kollias, P.; Lean, K.; Lori, M.; Mahfouf, J.-F.; Mello, S.; Midthassel, R.; Munro, Y.; Nicol, J.; Potthast, R.; Rennie, M.; Stein, T. H. M.; Tanelli, S.; Tridon, F.; Walden, C. J.; Wolde, M.

Publisher's version / Version de l'éditeur:
https://doi.org/10.1175/BAMS-D-16-0047.1
Bulletin of the American Meteorological Society, 2018-02-12

The DOI for this manuscript is doi: 10.1175/BAMS-D-16-0047.1

The final published version of this manuscript will replace the preliminary version at the above DOI once it is available.

If you would like to cite this EOR in a separate work, please use the following full citation:

Illingworth, A., A. Battaglia, J. Bradford, M. Forsythe, P. Joe, P. Kollias, K. Lean, M. Lori, J. Mahfouf, S. Mello, R. Midthassel, Y. Munro, J. Nicol, R. Potthast, M. Rennie, T. Stein, S. Tanelli, F. Tridon, C. Walden, and M. Wolde, 2018: WIVERN: A new satellite concept to provide global in-cloud winds, precipitation and cloud properties. Bull. Amer. Meteor. Soc. doi:10.1175/BAMS-D-16-0047.1, in press.

WIVERN: A new satellite concept to provide global in-cloud winds, precipitation and cloud properties.

A.J. Illingworth[*1], A. Battaglia[2], J. Bradford[3], M. Forsythe[4], P. Joe[5], P. Kollias[6], K. Lean7, M. Lori[8], J-F Mahfouf[9], S. Mello[5], R Midthassel[10], Y. Munro[11], J. Nicol[1], R. Potthast[1,12], M. Rennie[7], T.H.M. Stein[1], S. Tanelli[13], F. Tridon[2], C.J. Walden[3], M.Wolde[14].

Affiliations:

[1] Department of Meteorology, University of Reading, UK

[2]University of Leicester, Leicester, & National Centre for Earth Observation, UK.

[3]Science and Technology Facilities Council, UK

[4]Met Office, UK

[5]Environment and Climate Change Canada (ECCC), Canada

[6]Stony Brook University, Stony Brook, NY, USA

[7]European Centre for Medium-Range Weather Forecasts, Reading, UK

[8]HPS-GmbH Munich, Germany

[9]MétéoFrance, France.

[10]European Space Agency, European Space Research and Technology Centre, NL

[11]Airbus Defence and Space Limited, UK

[12]Deutscher Wetterdienst, Germany

[13]Jet Propulsion Laboratory, California Institute of Technology, USA

[14]National Research Council, Canada

* *Corresponding author address*: Anthony J. Illingworth, Department of Meteorology, University of Reading, Earley Gate, PO Box 243, Reading RG6 6BB, UK.

Tel: +44 118 378 6508

E-mail: a.j.illingworth@reading.ac.uk

ABSTRACT

This paper presents a conically scanning space-borne Dopplerized 94GHz radar Earth Science mission concept, WIVERN, 'Wind VElocity Radar Nephoscope'. WIVERN aims to provide global measurements of in-cloud winds using the Doppler shifted radar returns from hydrometeors. The conically scanning radar could provide wind data with daily revisits poleward of 50°, 50-km horizontal resolution and approximately 1km vertical resolution. The measured winds, when assimilated into weather forecasts and provided they are representative of the larger scale mean flow, should lead to further improvements in the accuracy and effectiveness of forecasts of severe weather and better focusing of activities to limit damage and loss of life. It should also be possible to characterize the more variable winds associated with local convection. Polarization diversity would be used to enable high wind speeds to be unambiguously observed; analysis indicates that artifacts associated with polarization diversity are rare and can be identified. Winds should be measurable down to 1 km above the ocean surface and 2 km over land. The potential impact of the WIVERN winds on reducing forecast errors is estimated by comparison with the known positive impact of cloud motion and aircraft winds. The main thrust of WIVERN is observing in-cloud winds, but WIVERN should also provide global estimates of ice water content, cloud cover and vertical distribution continuing the data series started by CloudSat with the conical scan giving increased coverage. As with CloudSat, estimates of rainfall and snowfall rates should be possible. These non-wind products may also have a positive impact when assimilated into weather forecasts.

CAPSULE (20-30 words)

A new satellite concept with a conically scanning W-band Doppler radar to provide in-cloud winds, together with estimates of global rainfall, snowfall and cloud properties.

According to the World Meteorological Organization (WMO), wind-storms are by far the largest contributor to economic losses caused by weather related hazards, resulting in approximately 500 billion USD (adjusted to 2011) of damage over the last decade globally (Zhang 2016). With more than 50% of the Earth's population concentrated in coastal developments and mega-cities, extreme weather events have an increasing potential to cause significant and recurring damage in terms of both loss of life and economic loss. As such, Disaster Risk Reduction has been singled out by the WMO as their number one strategic priority, highlighting the importance of improving the accuracy and effectiveness of forecasts and early warnings of high-impact meteorological environmental hazards (Zhang 2016). Baker et al. (2014) provide an excellent review of the need for global wind measurements and argue that the measurement of the three-dimensional global wind field is the final frontier that must be crossed to significantly improve the initial conditions for numerical weather forecasts, and quote WMO as determining that global wind profiles are "essential for operational weather forecasting on all scales and at all latitudes". Assimilation of additional wind observations from the 94 GHz radar on the proposed future WIVERN satellite into weather forecast models should significantly improve weather prediction skill allowing better focus of mitigation activities with respect to timing, location and assigning resources.

Particularly striking examples of the advantages of mitigation activities are the tropical storm "Nargis" that hit Myanmar in 2008, when no preventive action was taken and 138,000 died, and the subsequent more powerful storm "Phaillin" that struck the E Coast of India in October 2013 but caused only 43 fatalities because timely warnings were issued, and a mass evacuation of those living in the coastal regions was organized. In Europe, the windstorms in 1999 were estimated to have caused €18.5B of damage, and in 2009 on 24 January the very deep depression ‘Klaus’ caused 28 deaths through drowning as it crossed the coast of western France leaving 1.7 million people without electricity. A succession of rapidly deepening depressions forming over the western Atlantic crossed the UK during December 2015 and January 2016 with the heavy rain and flooding resulting in insurance losses of about €1.5B.

WMO has outlined the systematic observation requirements for satellite-based products (GCOS 2006) as part of their Rolling Requirements Review process and also maintains requirements in the Observing Systems Capabilities Analysis and Review tool (OSCAR 2016). The relevant numerical weather prediction (NWP) requirements for winds are summarized in Table 1. One conically-scanning WIVERN radar placed in Low Earth Orbit could measure the line-of-sight (LOS) component of the horizontal wind and should be able to satisfy the breakthrough requirements in Table 1 for in-cloud winds, except for the 6-hour observing cycle that would require multiple satellites. To achieve the observation requirements of having a fine vertical resolution and a short observing cycle, we currently envisage (Table 2) a 94 GHz (3.2 mm wavelength) radar with a 2.9 by 1.8 m elliptical antenna producing a narrow, conically scanning pencil beam at 38° off-nadir and 41° off-zenith at the surface with an orbit altitude of 500 km and a surface footprint of approximately 1 km in diameter. These parameters are chosen as a compromise between the need to have a higher orbit and thus a broader ground track to reduce the satellite revisit time, and the consequent requirement of a much larger antenna to maintain the 1 km vertical resolution when the slant path to the surface is increased. The 2.9 m elliptical antenna would have a beamwidth of 0.11° in the horizontal and 0.08° in the vertical, so, in combination with a 3.3 μs pulse length (500 m round-trip slant path), the vertical resolution (-3 dB) would be about

800 m assuming both the antenna beam pattern and pulse shape are Gaussian. 94 GHz is the preferred frequency as a 35 GHz radar would have a pencil beam 2.7 times wider with consequent loss of vertical resolution. As indicated by the sketch in Fig. 1, the antenna would rotate once every 7.5 seconds tracing out a circular ground track 800 km in diameter advancing 50 km for each revolution.

The WIVERN mission will be complementary to other observing systems providing unique insights into the structure of winds within clouds and precipitating systems. The impact on Numerical Weather Prediction (NWP) is expected to be on features in the models that are long-lasting when compared to the revisit times, so it will be necessary to identify convective motions that are not representative of the large-scale flow. The Aeolus Doppler wind Lidar satellite mission (Stoffelen et al. 2005) is expected to measure line-of-sight winds in clear air, through optically thin clouds/aerosol and from the top of optically thick clouds/aerosol, but it lacks the penetrating capability of a radar for measuring within most clouds. To improve NWP forecasts the need is for wind observations upstream of the areas were the wind damage may occur 24 to 48 hours later; McNally (2002) has shown that these 'meteorologically sensitive areas' are often cloudy. Fig. 2 shows the coverage expected in one day for the notional WIVERN configuration of a 500nkm orbit tracing out an 800 km diameter ground track that results in a revisit time of about once a day for latitudes poleward of 50° and more frequent visits over the polar regions. These regions have become an important area for climate and weather studies as demonstrated by the recently launched WMO "Polar Prediction Project" that aims to promote cooperative international research enabling development of improved weather and environmental prediction services for the polar regions. In the Arctic the fast warming, the decrease in ice cover and the recent opening of the Northwest Passage have attracted attention. The limited number of ground based profiling observations in the Arctic regions indicate the ubiquitous presence of light precipitation often limited to the lowest 4 km whose properties may be sensitive to the local and mid-latitude aerosol transported from mid-latitudes. WIVERN observations would provide pan-Arctic coverage and reveal the true physical and dynamic characteristics of the clouds and precipitation in these data sparse regions.

THE WIVERN CONCEPT AND PREDICTED DOPPLER PERFORMANCE.

WIVERN would utilize a 94 GHz transmitter similar to the one that has been operating beyond expectations on the nadir-pointing CloudSat Cloud Profiling Radar (Stephens et al. 2008, Tanelli et al. 2008) since its launch in 2006. CloudSat transmits 3.3 μs (500 m) pulses at a pulse repetition frequency (PRF) of approximately 4 kHz with 1800 W peak power (at beginning of life) and 24 W mean radiated power. By integrating the pulses for 0.16 s, equivalent to a distance of 1.09 km along track, during which about 600 pulses are transmitted, it was therefore possible during CloudSat's prime mission to detect targets with reflectivities above -30 dBZ and a single pulse signal-to-noise ratio (SNR) of 0 dB for an echo of ≈ -16 dBZ. The proven performance of CloudSat can be used both to estimate the accuracy of the retrieved LOS speeds from WIVERN, and the climatology of radar reflectivity profiles around the globe from several years of CloudSat data can be used to predict the number of occasions that WIVERN would observe accurate winds. An improvement in the sensitivity of WIVERN compared to CloudSat can be expected, because of the shorter slant path to the ground (≈ 650 km vs CloudSat's ≈ 710 km) and the larger antenna (1.8 m by 2.9 m for WIVERN vs CloudSat's circular 1.8 m). This should lead to a single pulse SNR of 0 dB for a return of ≈ -19 dBZ, and for integration lengths of 1, 5 and 10 km the reflectivity threshold for 0dB SNR will be -24dBZ, -27.5dBZ and -30.5dBZ, respectively.

The EarthCARE satellite (Illingworth et al. 2015) will use the conventional pulse pair technique to detect the nadir Doppler velocity of the hydrometeors, using a PRF of 7.5 kHz, so that only one pulse at a time is present in the troposphere, but this leads to a folding velocity of just 6m s^{-1} and a noisy Doppler estimate because of the low correlation of the phases of the pulse pair echoes. As explained in the sidebar, 'Why polarization diversity', WIVERN overcomes this dilemma by estimating the Doppler velocity using the polarization-diversity pulse-pair (PDPP) technique (Pazmany et al. 1999) and will transmit a pair of pulses one with horizontal polarization (H) the other with vertical (V), with a short separation, T_{hv}. A value of 20 μs is proposed for T_{hv} so that the folding velocity is 40 m s^{-1} and large enough to comfortably exceed the errors of the winds calculated in the NWP models. The pulse separation would be 3 km along the slant path or 2.3 km in the vertical.

WIVERN would trace out a quasi-circular ground track of diameter 800 km on the ground, advancing 50 km along track for each rotation with the footprint traveling at 335 km s^{-1} or 1 km in 3 ms. If it were to use the same 4 kHz PRF as CloudSat, in each km it could transmit 10 H-V pulse pairs each with a 20 μs separation to measure Doppler, interleaved with 2 single H or V pulses to measure the LDR of the targets to flag any potential problems of cross talk between the two polarizations. The ten pulse pairs would alternate between H-V and V-H to distinguish between phase shifts due to Doppler and to differential phase shift on backscatter (Pazmany et al. 1999). The predicted Doppler accuracies for 1, 5 and 20 km integrations are displayed in Fig. 3. The measured sight component (LOS) of the wind can be converted to the horizontal line-of sight winds (HLOS) winds if the vertical wind component is assumed to be zero. To satisfy the WMO requirement of a horizontal wind component (HLOS) of 2 m s^{-1} an LOS wind accuracy of 1.35 m s^{-1} is needed, this can be achieved for 20 km integration if the echoes are > -20 dBZ, and for 5 km they should be above -15 dBZ, provided there are no ghosts caused by cross talk between H and V returns. Note that factors such as beam pointing knowledge and non-uniform beam filling (discussed later) may well prevent the theoretical accuracies < 0.5 m s^{-1} being achieved for the higher dBZ values.

To gauge the number of sufficiently accurate wind observations expected from the proposed WIVERN satellite and their susceptibility to ghosts, an analysis of reflectivity profiles averaged over a 20 km along track integration for four years of CloudSat data is displayed in Fig. 4. The upper panel shows that, averaged over the tropics and northern mid-latitudes, clouds with echoes > -20dBZ are present for about 10% of the time between heights of 1 and 10 km, and this fraction does not change markedly for reflectivity thresholds of -25, -20 and -15 dBZ. These figures are for 20 km integration but change by less than 0.2% for shorter integrations down to 1 km. For clouds 10 km deep, the sloping WIVERN sample at cloud top will be displaced by 7 km horizontally compared to the ground footprint, the insensitivity of the CloudSat statistics to the integration length suggests that this horizontal displacement and areas of broken cloud will not bias the WIVERN observations. The vertical resolution of WIVERN winds should be better than 1km, so, for a 20 km integration and before thinning, on average one wind with an accuracy better than 2 m s^{-1} (HLOS) should be detected every 60 ms or 1.4 million per day.

'Ghost' echoes caused by cross-talk between the H and V returns may occur when there are high reflectivity depolarizing targets 2 km above or below much weaker targets. The phases of the ghost echo are uncorrelated with the true return signal so their effect will be to increase the random error in the velocity estimate at each gate; this may occur over several neighbouring gates but these random errors should not introduce any bias as the ghost echoes decorrelate between successive pulse pairs. The lower panel in Fig. 4 is a plot of CloudSat observations for each height level, 'h', of the fraction of the time that there is a denser cloud with a reflectivity 20 dB greater at a height either 2 km above or below 'h'. For clouds with reflectivities above -15 dBZ this occurs about 2% of the time. As a worst case we assume that the LDR of the denser clouds is -15 dB, then on 2% of occasions there would signal-to-ghost ratio (SGR) of -5 dB; Fig. 3 shows that the LOS velocity accuracy of 1.35 m s^{-1} could still be achieved for 20 km integration for dBZ > -10dBZ. We conclude that significant ghost echoes from hydrometeor returns should be rare. In the next section we will present some observations to support this conclusion. We will also consider the more serious problem of ghost echoes and biases in the velocity estimates in gates close to the surface as a result of surface clutter, and the biases due to both the vertical wind shear and by the satellite motion when there is non-uniform beam filling.

If the winds from WIVERN are to be assimilated it will be necessary to identify regions where LOS winds are affected by convection and are not a representative component of the large-scale horizontal wind. Anderson et al. (2005) have analyzed aircraft observations of tropical convection and define an updraft core as a region of diameter > 500 m having a vertical velocity > 1 m s^{-1} and find that 90% of such cores have diameters of less than 3 km in diameter. One year's continuous observations of profiles of vertical velocity and reflectivity made with the zenith-pointing 35 GHz cloud radar at Chilbolton, UK, confirm that regions of up and down drafts exceeding 1 m s^{-1} are absent in stratiform clouds, and confined to convective regions where the reflectivity values exceed +10 dBZ. From Fig. 3 we conclude that the LOS velocity should be accurate to 1.35 m s^{-1} for each km along the ground track provided Z is above -5 dBZ. We propose that convective regions should be identified by significant changes in LOS velocities on the km scale and flagged as non-representative for global NWP data assimilation users. These fluctuations of the observed LOS velocities should be of interest to those studying the characteristics and statistical properties of convective processes and for validating cloud-resolving models. The detailed evolution of individual convective clouds cannot be observed from a single satellite in low earth orbit so such studies are best conducted from aircaft.

GCOS has recently recommended (GCOS, 2017) a satellite be launched to continue the data set that CloudSat has been gathering on cloud reflectivity profiles since its launch in 2006 and to be continued by EarthCARE. WIVERN should be able to provide such data. Miller and Stephens (2001) show that a minimum detectable signal of -28 dBZ should detect a fraction of the true cloud field sufficient to reconstruct the instantaneous top-of-the atmosphere to within Clouds of the Earth's Radiant Energy system (CERES) requirements. WIVERN should achieve -27.5 dBZ sensitivity for 5km along ground track integration (50 pulse pairs) corresponding to 15 ms integration time; whereas CloudSat and EarthCARE will have a 5km nadir along track reflectivity sample about every 0.8 s suggesting that WIVERN would obtain about a fifty fold increase of IWC profiles.

The hydrometeor cloud targets are not perfect tracers of the wind, so a correction would be needed to account for their terminal velocity. Battaglia and Kollias (2015) reported that the error in the mean terminal velocity of ice clouds is a function of their reflectivity and is < 0.2 m s^{-1} up to 10 dBZ and that the random error for Z < -5 dBZ is 0.5 m s^{-1}; this should introduce a random error of < 1 m s^{-1} into the inferred horizontal component of the wind. For rainfall at 94 GHz Mie scattering by the larger raindrops leads to a Doppler velocity of about 4 ± 1 m s^{-1} (Lhermitte 1990) so a correction accurate to < 1m s^{-1} of the HLOS winds should be achievable. When the radar gate straddles the melting layer, the terminal velocity changes rapidly, but such occasions can be flagged by the high values of the depolarization ratio, LDR, resulting from the irregular rocking motion of the wet oblate melting snowflakes.

POTENTIAL SPURIOUS SIGNALS FROM THE DOPPLER RADAR.

Ground clutter. Surface clutter contamination can affect the hydrometeor Doppler signal; if the signal to clutter ratio (SCR) is 15 dB it will lead to a 3% bias of the hydrometeor velocity towards the surface zero velocity. The shape of the clutter signal is determined by the combined effect of the WIVERN antenna pattern, its pulse-shape, and the illumination geometry while its intensity is driven by the surface backscattering properties (Meneghini and Kozu 1990). A recent aircraft campaign funded by ESA and conducted in Canada using the NRC Airborne W-band radar has characterized the surface return at WIVERN incidence angles (41^0) both for ocean and flat land surfaces (full details in Battaglia et al. 2017). Over ocean the normalized backscattering cross sections (σ_0) are over 30 dB smaller than at nadir with typical values of -25 dB but roughly ranging between -35 dB and -15 dB with larger (smaller) values in presence of strong (weak) wind and when looking upwind (crosswind). Sea surfaces are moderately depolarizing at such angles with an LDR about -15 dB. Ocean backscattering properties are characterized by a strong angular dependence but land surfaces are more constant with σ_0 of the order of -10 dB. Forest-covered and rural surfaces present very similar results, whilst urban surfaces generate slightly higher values of σ_0.

The clutter expected for a WIVERN configuration when observing a flat surface with σ_0=0 dB is illustrated in Fig 5a for the WIVERN antenna pattern which was derived in the ESA-DORA ITT study (inset of Fig. 5b). The first antenna sidelobe at 0.15^0 is 20 dB below the maximum are clearly affecting the surface clutter above 1 km altitude. Clutter signals scale with σ_0 and are therefore expected to be about 10 dB (25 dB) lower than those depicted in

Fig. 5a over flat land (the ocean). If snow-covered surfaces have σ_0 lower than 0 dB (still to be determined by observations) the plot in Fig. 5a suggests that it will be possible to produce snow retrievals similar to CloudSat, with clutter contamination only in the last km close to the surface for Z_{snow} > -10 dBZ, and at lower altitudes for higher reflectivities. LOS winds must be derived only in regions with large signal-to-clutter ratios (15 dB or above). For reflectivities 3dB above the minimum detection threshold this means that the surface signal must be lower than -30 dBZ. For characteristic values of sea and land σ_0 this seems to be achievable at heights above 1 and 2 km, respectively

Cross polarization interference and the effect of "ghost" echoes. The ability of the polarization diversity scheme to derive wind velocities relies on limiting the coupling between the polarizations both at the hardware level typically reducing values to < -25 dB, while the wave propagates and scatters in the atmosphere. At the WIVERN incidence angles, atmospheric targets like melting hydrometeors and columnar crystals can produce LDR up to -12 dB (Wolde and Vali 2001) whilst surface clutter tends to depolarize more over land (LDR values of -9±3 dB) than over sea (characteristic value of -15 dB, Battaglia et al. 2017). The effect of cross-polarization is to produce an interference signal in each co-polar channel depending on the temporal shift between the H and V pair and the strength of the cross-polar power (which is given by the product of the LDR and the co-polar power) and appear as ``ghost echoes'' (Battaglia et al. 2013). The phases of ghost echoes are incoherent with respect to the echoes of interest so do not bias the velocity estimates, but increase their random error as a function of the signal to ghost ratio (SGR) (Pazmany et al. 1999); as illustrated by the dashed lines in Fig. 3 when the SGR falls to 0 and -5 dB this random error increases rapidly for shorter integration lengths. By replacing two in ten of the pulse pairs by a single H or V pulse, the LDR of the targets can be monitored and used to flag occasions when there may be cross talk between the H and V echoes.

Figure 6 shows simulated WIVERN observations of reflectivity and LDR of a stratiform precipitating system over the Pacific observed on the 10 January 2008 reconstructed by tilting and wrapping the vertical CloudSat curtain so as to be along the WIVERN scanning direction. CloudSat effective reflectivity and attenuation are derived from the 2C-RAIN product. The reconstruction accounts for the WIVERN observation geometry, its antenna pattern and assumes a 5 km integration length. LDR values sampled from normal distributions are used for rain, ice crystals, melting layer particles and mixed-phase clouds, with means of -23, -19 –14 and -17 dB and standard deviations of 2, 1.5, 1.5 and 1.5 dB, respectively. These values have been selected based on a climatology collected at the Chilbolton Observatory. Clutter with the shape shown in Fig. 5a and representative of flat land surfaces, having σ_0 normally distributed with mean value of -8 dB and standard deviation 4 dB, has been included. The reflectivity (panel a) clearly shows a region of strong attenuation in correspondence to the precipitation core (~2-6 mm h^{-1}) located around 600 km. The black line contours the region where Doppler velocities estimates are expected to have accuracies better than 2 m s^{-1} when adopting a T_{hv} equal 20 µs. The SCR is typically >20 dB (magenta line) for heights above 2 km where bias in velocities will be negligible. Ghost echoes (see sidebar 2) are expected when the SGR is < 3dB (yellow line in right panel) and are confined to the high reflectivity gradients at the cloud boundaries (where Doppler will be too noisy anyway) and close to the surface (that would be much reduced over the sea).

A month of CloudSat data (Jan 2008) have been used to simulate WIVERN profiles and the ghosts generated by T_{hv} values of 5, 20 and 40 µs taking into account the SNR, the SGR, and the SCR for each 5 km along track integration length in order to assess the fraction of profiles for which WIVERN is expected to produce winds with accuracy better than 2 m s^{-1} (Fig. 7. The fraction is much lower for the 5 µs T_{hv} values because the increased noise error maps into a large velocity error. Overall Fig. 7 shows that in the mid-troposphere (3-8km) WIVERN would provide a useful measurement 10% of the observation time, but reduced to 5% over land at heights near to 2 and 4km where the bright land surfaces produce ghost echoes for T_{hv} of 20 and 40 µs, respectively, indicating that 20 µs may be optimum.

Ground-based validation of theoretically predicted wind errors and biases. The degree to which ghost echoes and/or vertical gradients in reflectivity combined with vertical wind shear can lead to increased random errors or biases in the wind estimates made from space by WIVERN, can be assessed using recent observations made with the 94 GHz radar at Chilbolton in Southern England pointing 45° off-zenith with a time resolution of six seconds and gate length of 60 m. The case of 27 June 2017 (Fig. 8, panels A to D) is chosen because of the large gradient in received power exceeding 20 dB for the 3 km/20 µs separation of the H-V pulse pair (panel A); this will lead to signal to ghost (SGR) ratios of 0 dB and -5 dB for LDR values of -20 dB and -15 dB (not shown – but in the melting layer at 4 km range they reached -15 dB resulting in the SGR of -5 dB at 7.5 km range). The velocity estimated with T_{hv} = 20 µs (panel C) at a height of 4.54 km where SGR is at its lowest is plotted in black in panel D (upper trace) whereas the 'true' velocity from the H-H pulse pairs separated by 160 µs (when there will be no ghost echoes) is in red; the increased gate-to-gate random noise introduced by the ghosts in the black trace when SGR is low is very clear when compared to the smooth red trace. The lower trace in panel D shows that the observed increases in the rms error for a T_{hv} = 20 µs agree very well with two independent theoretical predictions of the error (see Fig. 3); one based on the SNR and SGR computed via the LDR estimate, and a second based on the drop in observed correlation between the H-V returns due to the increase in the noise. This plot confirms that ghosts increase the random error of the wind estimate but do not introduce any bias. Ghosts are observed relatively frequently from the ground, because of the ~10 dB change in received power from the same target at a range of 1 km and 3 km. so they are useful for validating the theory, but ghosts should be much less frequent from space, because of the negligible fractional change in range of the targets (see Fig. 4b). Biases in the radar-derived winds may arise when there is a vertical wind shear that coincides with a large vertical gradient of radar reflectivity; this is the case in panels A and C where at a slant range of 4.5 km the reflectivity across the bright band changes by 10 dB in 1 km and the vertical wind shear is about 5 m s^{-1}. These radar observations are taken every six second with a gate length of 60 m. From the average winds at this resolution, the true velocity for a WIVERN sample volume of 800 m length by 10 minutes (equivalent to a horizontal distance of 10km from the satellite if the horizontal advection velocity is 1 km min^{-1}) can be computed and the bias derived by comparing this 'true' velocity with the reflectivity weighted mean velocity that would be detected by WIVERN. From this image WIVERN would obtain 550 wind samples with an rms LOS wind error of 0.16 m s^{-1} and an average bias of 0.07 m s^{-1}, but for data assimilation purposes the data would be thinned. The case above was chosen because of the marked bright band, but panels E and F illustrate the case of 28 Aug 2017 when a region of wind shear of 20 m s^{-1} per km and reflectivity gradients of up to 20 dB km^{-1} descended by 2-3 km in 10 hours. The biases can also be predicted from changes in velocity from neighboring samples at the WIVERN resolution and the observations rejected when this exceeds 0.3 m s^{-1}. The result is that ~ 20% of the WIVERN samples are rejected, and the remaining WIVERN observations have a bias of 0.05 m s^{-1} and an rms error of 0.34 m s^{-1}.

Non-Uniform beam filling (NUBF). For fast-moving space borne Doppler radar, reflectivity gradients within the radar sampling volume can introduce a significant source of error in Doppler velocity estimates (Tanelli et al. 2002). When adopting slant-viewing geometry the situation is illustrated in Fig. 5b, with the shading of the WIVERN sampling volume indicating the strength of the backscattered signal. The red and green arrows indicate the apparent velocity introduced to the WIVERN volume due to the motion of the satellite (green toward and red away from the satellite); as a result, for the case illustrated, a downward bias will be produced. Notional studies have demonstrated that such biases can be mitigated by estimating the along-track reflectivity gradient (Schutgens 2008, Kollias et al. 2014; Sy et al. 2014). For WIVERN the relevant gradients are those along the direction in the plane generated by the satellite velocity and by the antenna boresight and is orthogonal to the latter (identified by η in Fig. 5b). As a consequence, NUBF effects are linked to reflectivity gradients along different directions depending on the scanning position of the rotating antenna, with NUBF velocity biases expected to be linearly proportional to such reflectivity gradients with a coefficient of the order of 0.1-0.15 m s^{-1} dB^{-1} km (Battaglia and Kollias 2015). When side-looking, the relevant reflectivity gradients are those along-track, which can be estimated from the reflectivities measured along the scanning track and used to mitigate the NUBF effect. However, such mitigation is increasingly less feasible when moving from side to forward/backward-looking angles where the relevant reflectivity gradients correspond to a direction that is orthogonal to the scanning track. However, thanks to the WIVERN conical scanning geometry, on average, the biases looking in opposite directions with respect to the satellite motion cancel out and NUBF leads only to an increase in the random error of the wind. A high-resolution (0.5 km horizontally and 0.3 km vertically) synthetic reflectivity field obtained from a WRF simulation of hurricane Isabel has been used to estimate the NUBF-induced errors of WIVERN measurements. Preliminary results show that errors should be less than 0.5 m s^{-1} for side-looking and 2 m s^{-1} for forward/backward-looking angles. More work is needed in order to properly characterize the variability of the wind and of the 94 GHz reflectivity field at the WIVERN sub-pixel scale. Data sets obtained via airborne of ground-based 94 GHz Doppler radars could be used to test the detrimental NUBF effect on Doppler measurements.

Pointing Accuracy. The rotating antenna will introduce a sinusoidal component of the satellite velocity with an amplitude of about 5,000 m s^{-1}. If the bias is to be less than 0.5 m s^{-1} then the radar electrical boresight elevation and azimuthal angles should be known to < 100 μrad. If the radar is used as an altimeter, the elevation angle can be continually monitored by measuring the range as the antenna scans over the sea; for a slant range of 651 km, an error of 100 μrad would manifest itself as an apparent change in range of the sea surface of 42 m. For a point target with an SNR> 20 dB, Skolnik (1981, page 402) shows that changes in the time of the leading edge of the return echo can be estimated to within 5% of the echo rise time; simulations using distributed scatterers on the sea surface confirm that this accuracy can be maintained by averaging 100 pulses (10 km along the ground track). Turning to the requirement to know the azimuthal angle to 100 μrad, equivalent to a distance along the scanning ground track of just 65 m, or about one tenth of the beamwidth, an error of 100 μrad in pointing knowledge will result in a sinusoidal velocity error with maxima of ± 0.5 m s^{-1} when pointing across track. More studies are needed on this topic, but we propose two approaches. Firstly, when pointing precisely across track ground clutter will appear to be stationary and averaging over many scans should identify the precise angle at which this happens, and, secondly, we will use regions of light winds where the ECMWF analysis provides winds accurate to better than 1 m s^{-1} to make small adjustments to the azimuthal pointing knowledge to remove the systematic biases when pointing across track..

Multiple scattering. When dealing with space-borne millimetric radars, in the presence of highly attenuating media, the multiple-scattering signal can overwhelm the single scattering contribution (Battaglia et al. 2010) with very detrimental effects both on retrieval and Doppler products (Battaglia and Kollias 2014). Studies based on CloudSat have demonstrated that multiple scattering is not negligible in the presence of high-density ice (hail and graupel) or moderate/intense rain, (Battaglia et al. 2011). With an LDR mode, segments of the profiles affected by multiple scattering can be easily flagged (e.g. by the condition LDR>-10 dB, see Battaglia et al. 2007) and excluded from further wind analysis. Indeed air motions in these conditions would not be assimilated into the model even if they had been properly retrieved, as they are not representative of the large scale flow and are transient features compared to the revisit time of the satellite.

THE IMPACT OF WIND OBSERVATIONS ON GLOBAL NWP MODELS.

The main impact of the WIVERN wind observations should be realized through their assimilation into global NWP models. The 'Forecasting Sensitivity to Observations', 'FSOI' technique (Langland and Baker 2004), implemented in the ECMWF model by Cardinali (2009), is a very powerful tool that enables, for the first time, quantification of the impact of individual observations that are assimilated in to the NWP forecast model in reducing the "forecast error" obtained by comparing the T+24 forecasts of temperature, wind, humidity and surface pressure with their corresponding analyses. The contributions of the top five observation types in reducing this forecast error for the Met Office, ECMWF and MétéoFrance global models are displayed in Table 3. This shows that both the in-situ aircraft observations and the "Atmospheric Motion Vectors" (AMVs, the winds derived from the movement of cloud or water vapour features in successive satellite images), make an important contribution to reducing forecast errors, second only to the humidity and temperature structure provided by the IR and microwave sounders.

The initial high resolution AMV wind observations are thinned in the ECMWF global model to provide, at most, a single wind estimate for each 200 by 200 km horizontal 'box', a vertical thinning of 50-175 hPa that varies with height, and a 30 minute temporal thinning. This thinning is to account for the spatial and temporal correlation of AMV winds errors over large distances due to errors in the height assignment. The figures for the Met Office are similar: 200 by 200 km, 100 hPa and two hours. ECMWF blacklist AMV winds over land below 500 hPa, while the Met Office is not quite so strict with a height limit over land usually closer to 600 hPa north of 20°N. If observations are assimilated at too high a horizontal density, the fact of not accounting for spatial correlations of observation errors in the analysis can also degrade the resulting forecasts (Liu and Rabier 2002). Aircraft winds do not suffer from problems associated with strong spatial correlations and screening over land, and in the ECMWF model are used for a height range that extends down to within 1 km of the surface and are currently thinned to 70 km in the horizontal and 15 hPa; this will be reduced to 35 km and 7.5 hPa in 2018. Currently, about half of all aircraft winds are below 500 hPa. The case studies discussed in Fig. 8 suggest that the radar-derived winds should have similar error characteristics to aircraft winds but may be rather larger because of their 800m vertical resolution.

Table 4 compares the contributions of the AMV winds and the in-situ aircraft measurements to the ECMWF global model and shows that when AMV winds are assimilated they are, on average, assigned a random error of 4.6 m s^{-1} for the zonal component of the wind, but for the in-situ aircraft winds the error is only 2.3 m s^{-1}. Combined with the larger thinning of the AMV winds, the net result is that only 4% of the AMV observations are assimilated as opposed to 36% of the aircraft observations. The CloudSat analysis summarized in Figs. 4 and 7 indicates that about 1.3 million winds with a resolution of 20 km along track would be obtained each day. If these were thinned to 50 km, similar to the ECMWF value planned for aircraft winds in 2018, then the number assimilated could be about 500,000 per day. By comparison with the figures in Table 4, this suggests that their impact on the forecast should be significant.

The winds from WIVERN are only line of sight but Horányi et al. (2015a) have demonstrated that, with a state of the art data assimilation system and real observations, HLOS winds such as would be obtained from an aircraft provide about 70% of the impact of a vector wind, and that in the tropics the impact of wind data is much greater than the mass information. McNally (2002) provides further evidence for the potential impact of in-cloud winds. He investigated the sensitivity of the weather forecasts to errors in the analysis of the current atmospheric state that subsequently develop into significant medium-range forecast errors. The main obstacle was the presence of cloud in these ‘sensitive’ areas; depending on the amount and altitude of cloud cover the information from infrared (IR) sounders (advanced or otherwise) could be severely limited.

If winds are to be assimilated it is extremely important that the systematic errors of the observations are not too large relative to the random errors. Simulations carried out to predict the potential impact of the winds from the Aeolus satellite by Horanyi et al. (2015b) have shown that assimilating winds that are biased by 1-2 m s^{-1} when the random error standard deviation is around 2 m s^{-1} will actually degrade the forecast unless the bias can be estimated and removed prior to assimilation. Our analysis suggests that winds from WIVERN should only be biased when they are affected by ground clutter and that such regions should be easy to identify.

The mean observation error and the number of AMV winds from Meteosat 10 that were assimilated into the Met Office model for the month of December are plotted in Fig. 9. The AMV error is a combination of error in the tracking step and an error in speed due to an uncertainty in the height assignment as discussed by Salonen et al. (2012); Forsythe and Saunders (2008) describe how the assigned AMV velocity error increases with the vertical wind shear in the model. For heights above 500 hPa and for all latitudes, the mean observation error is mostly in the range 5 to 9 m s^{-1}. The maximum number of assimilated winds is found at around 900 hPa over the Southern Oceans, followed by heights of 200-400 hPa at all latitudes, with a lower number of winds in mid-levels. The vertical distribution of ECMWF assimilated winds is also bimodal with fewer winds between 400 and 700h Pa. Analysis of CloudSat data (Figs 4and 7) suggests that one advantage of the WIVERN winds should be the absence of the current mid-level gap in coverage.

The actual numbers of AMV U-component winds assimilated into the ECMWF model during a 12-hour cycle in October 2016 are displayed in Fig 10 for each 10° by 10° area over the globe. The numbers are expressed as the number of observations per 10^6 km^2 area with the data having been thinned to 200 by 200 km 'boxes' in the horizontal, so that along the equator, a value of 100, would be equivalent to 4 winds per box in the 12 hour period. When predicting the performance of WIVERN we assume a thinning to 80km, close to the current ECMWF value for aircraft winds, and use the CloudSat data to calculate for every 80 km along-track segment how often there is a cloud echo of at least 5km length where the reflectivity exceeds -18 dBZ, for which (from Fig. 3) we expect the velocity error to be less than 2 m s^{-1}. CloudSat has only a small footprint at nadir, so to simulate the 800km wide circular ground path, we multiply these numbers by 11, and calculate on average the number of winds per 10^6 km^2 area in a 12 hour period as displayed in Fig. 10. This Fig. indicates that the number of WIVERN winds assimilated should be of similar magnitude to the current AMV winds.

Recent experience at Météo-France has shown that increasing the vertical resolution of observations in the 4D-Var data assimilation system of the global ARPEGE NWP model, has always had a positive impact in terms of analyses and forecasts, even though vertical correlation errors are neglected. One example is the increase of vertical resolution of GNSS-Radio-Occultation (RO) bending angle measurements obtained from limb sounding instruments. For each occultation, about 200 measurements are available between 50 km and the Earth's surface, and when the number assimilated was increased by a factor of 4, the fit of the model to the observations was improved both in the analyses and in the short-range forecasts of the model. A second study involved the impact of high-resolution radio sondes when the sonde data were sampled to reflect the vertical grid of the ARPEGE model, and again there was a better fit of the model to the observations both for the analysis and the background. These findings indicate the additional benefit to NWP from an active radar providing profiles of winds at each km height level through clouds, rather than a single wind measurement from near cloud top from passive sensors.

ADDITIONAL PRECIPITATION AND CLOUD PRODUCTS.

The main thrust of the WIVERN mission is to provide winds, but the satellite would also measure profiles of reflectivity over the 800 km wide ground track. CloudSat, with its approximately 1 km nadir-only footprint, has provided a unique cloud and IWC climatology that has been invaluable for validating NWP and climate models (e.g. Li et al. 2012) and also the best climatology of light rainfall over the oceans (e.g. Berg et al. 2010; L'Ecuyer and Stephens, 2002; Haynes et al. 2009). The rainfall is estimated by measuring the attenuation of the ocean surface return for the nadir pointing CloudSat; but for WIVERN the ocean surface return at 41° incidence is much lower, so heavy rain will totally attenuate the surface return, and rainfall estimates will probably be restricted to lighter rainfall. Much of the snowfall over polar regions has values of Z well below 20 dBZ and cannot be detected by the radars on the GPM satellite, but, with its sensitivity limit of -30 dBZ, CloudSat has provided the best global snowfall climatology to date (e.g. Liu 2008; Palerme et al. 2014). The performance of WIVERN for measuring snowfall will depend critically on the level of ground clutter and the radar reflectivity of the snow (see Fig. 5). More work is required to establish the accuracy and errors of rain and snowfall rates from WIVERN. Finally Janiskova et al. (2012) and Janiskova (2015) have demonstrated that the assimilation of CloudSat reflectivities into the ECMWF model has a slight positive impact on the subsequent forecast; we can expect a 50-fold increase in coverage from the 800-km wide ground track of WIVERN.

CHALLENGE AND SUMMARY

We expect that the proposed polarization diversity Doppler radar for WIVERN would be able to provide the horizontal component line-of-sight winds with an accuracy of 2 m s^{-1}, 50-km resolution in the horizontal and < 1km resolution in the vertical over an 800-km wide ground track, for clouds having a 20 km along track extent and a reflectivity exceeding -20 dBZ. Previous studies suggest that line-of-sight winds have 70% of the value of full vector winds (Horanyi et al. 20015a) and that 'sensitive' areas where observations are needed to improve forecasts are often cloudy (McNally 2002). Preparatory mission studies confirm that any artifacts associated with the polarization diversity technique should be rare and can easily be identified and rejected. Recent radar observations from aircraft suggest that ground clutter may introduce a bias into winds being measured below 1 km over the ocean and 2 km over the land, but more studies are needed to establish their magnitude and frequency of occurrence; knowledge of these boundary layer winds may be less crucial for 24 or 48-hour forecasts. Analysis, using the global climatology of cloud echoes obtained from CloudSat, indicates that the number of winds suitable for assimilation into operational weather forecasts should be comparable with the currently available aircraft winds and have similar error characteristics and so should have a significant impact in reducing forecast errors. At present there is a lack of wind observations between 400 and 700 hPa; analysis suggests that WIVERN should not suffer from this mid-level gap in coverage. Recent ground based polarization radar observations indicate that ghost echoes lead to increased random errors of the wind estimates but should be rare and can be identified and flagged, and that biases in wind estimates due to reflectivity gradients in the presence of wind shear can also be identified and should be < 1 m s^{-1}. Further airborne and ground-based studies are needed to confirm these results and to obtain and a more precise estimate of the occurrence of degraded winds due to non-uniform beam filling, and the extent of the blind zone over the ocean, and different land surfaces. It should be possible to identify areas of significant convection by the variability of the line of sight winds on the km-scale; such regions will not be suitable for assimilation into global forecast models but should provide statistical characteristics of convective motions. The WIVERN configuration with a 800 km wide ground track would use a similar transmitter to the one that has been operating well above expectations over the last decade on CloudSat, and would rely on well established polarization diversity techniques for deriving Doppler velocities and a 2.9 by 1.8 m 94 GHz antenna comparable in size to the antenna developed in a recent ESA study.

ACKNOWLEDGEMENTS

We thank the National Research Council of Canada Convair Aircraft flight crew for conducting the project flights, Cuong Nguyen for data processing and Andrew Pazmany of ProSensing for the implementation of the PDPP mode on the NRC Airborne W-band Radar. We acknowledge access to the Chilbolton Facility for Atmospheric and Radio Research funded by the Natural Environment Research Council in the UK. The work performed by S. Tanelli was carried out at Jet Propulsion Laboratory, California Institute of Technology under a contract with the National Aeronautics and Space Administration. Support from the CloudSat Project, Precipitation Measurement Missions program and NASA Weather Focus Area are gratefully acknowledged. We also benefitted from support by ESA contracts 4000113508 "Dual Polarization 94GHz antenna for Spaceborne Doppler Radar" and 4000114108 "Doppler Wind Radar Demonstrator' and CEOI-UKSA contract RP10G0327E13.

REFERENCES

Andersen, N.F., C.A. Grainger, and J.L. Smith, 2005: Characteristics of strong updrafts in precipitation systems over the central tropical Pacific ocean and in the Amazon. *J. Appl. Met.*, **44**, 731-738.

Baker, W.E., and Coauthors, 2014: Lidar-measured wind profiles: The missing link in the global observing systems. *Bull. Amer. Meteor. Soc.,* **92**, 543-564.

Battaglia, A., M. O. Ajewole and C. Simmer, 2007: Evaluation of radar multiple scattering effects in Cloudsat configuration. *Atmospheric Chemistry and Physics*, **7**, 1719-1730.

Battaglia, A., and Coauthors, 2010: Multiple scattering in radar systems: a review. *J. Quant.*

Spec. Rad. Transf., **111** (6), 917-947.

Battaglia, A., T. Augustynek, S. Tanelli and P. Kollias, 2011: Multiple scattering identification in spaceborne W-band radar measurements of deep convective cores. *J. Geophys, Res.,* **116**, D19201, doi:10.1029/2011JD016142.

Battaglia A., S. Tanelli, and P. Kollias, 2013: Polarization diversity for millimeter space-borne Doppler radars: an answer for observing deep convection? *J. Atmos. Ocean Technol.*, **30**, 2768–2787, doi: http://dx.doi.org/10.1175/JTECH-D-13-00085.1.

Battaglia, A., and P. Kollias, 2015: Using ice clouds for mitigating the EarthCARE Doppler radar mispointing. *IEEE Trans. Geo. Rem. Sens.,* **53**, 2079-2085m doi: 10.1109/TGRS.2014.2353219.

Battaglia, A. and P. Kollias, 2015: Error analysis of a conceptual cloud doppler stereoradar with polarization diversity for better understanding space applications. *J. Atmos. Ocean Technol.*, **32**, 1298–1319, doi: http://dx.doi.org/10.1175/JTECH-D-14-00015.1.

Battaglia, A., S. Wolde, L. Pio D'Adderio, C. Nguyen, F. Fois, A.J. Illingworth, and R. Midthassel, 2017: Characterization of surface radar cross sections at W-band at slant angles. *IEEE Trans. Geo. Rem. Sens.,* **55**, 3846-3859.

Berg, W., T. L'Ecuyer, J. M. Haynes, 2010: The Distribution of Rainfall over Oceans from Spaceborne Radars. *J. Appl. Met. and Climatol*, **49,** 535-543 doi: 10.1175/2009JAMC2330.1.

Cardinali, C., 2009: Monitoring the observation impact on the short-range forecast. *Q. J. R. Meteorol. Soc.* **135**: 239–250. doi: 10.1002/qj.366.

Forsythe, M., R. Saunders, 2008: AMV errors: a new approach in NWP. Proceedings of the 9th International Wind Workshop, Annapolis, Maryland, USA, 14-18 April 2008.

GCOS, 2006: Systematic observation requirements for satellite-based products for climate. http://www.wmo.int/pages/prog/gcos/Publications/gcos-107.pdf.

GCOS, 2017: 22nd Session of the GCOS/WCRP Atmospheric Observational Panel for Climate. https://www.wmo.int/pages/prog/gcos/AOPC-22/Report-Exeter-AOPC-22_final.pdf.

Haynes, J.M., and Coauthors, 2009: Rainfall retrieval over the ocean with spaceborne W-band radar. *J. Geophys, Res.*,**114**, doi:10.102/2008/D009973.

Hor´anyi, A., C. Cardinali, M. Rennie and L. Isaksen, 2015a: The assimilation of horizontal line-ofsight wind information into the ECMWF data assimilation and forecasting system. Part II: The impact of degraded wind observations. *Q. J. R. Meteorol. Soc.*, **141**, 1233-1243. doi: 10.1002/qj.2551.

Hor´anyi, A., C. Cardinali, M. Rennie, L. Isaksen L. 2015b: The assimilation of horizontal line-ofsight wind information into the ECMWF data assimilation and forecasting system. Part II: The impact of degraded wind observations. *Q. J. R. Meteorol. Soc.*, **141**, 1233-1243. doi: 10.1002/qj.2551.

Illingworth, A. J., and Coauthors, 2015: The EarthCARE satellite: The next step forward in global measurements of clouds, aerosols, precipitation and radiation. *Bull. Amer. Meteor. Soc.,* **96**, 1311-1332. doi: http://dx.doi.org/10.1175/BAMS-D-12-00227.1.

Janisková, M., P. Lopez and P. Bauer, 2012: Experimental 1D + 4D-Var assimilation of CloudSat observations. *Q. J. R. Meteorol. Soc.,* **138**, 1196–1220.

Janisková, M., 2015: Assimilation of cloud information from space-borne radar and lidar: experimental study usinga 1D+4D Var technique. *Q. J. R. Meteorol. Soc.,* **114**, 2708-2725. doi:10.1002/qj.2558.

Kollias, P., S. Tanelli, A. Battaglia and A. Tatarevic, 2014: Evaluation of EarthCARE Cloud Profiling Radar Doppler Velocity Measurements in Particle Sedimentation Regimes. *J. Atm. Ocean. Tech.*, **31**, 366-386.

Langland R., and N.L. Baker, 2004: Estimation of observation impact using the NRL atmospheric variational data assimilation adjoint system. *Tellus,* **56A,** 189-201.

Liu, G., 2008: Deriving snow cloud characteristics from Cloudsat observations. *J. Geophys. Res*., **113**, D00A09, doi:10.1029/2007JD009766.

Liu, Z.-Q., and F. Rabier, 2002: The interaction between model resolution, observation resolution, and observation density in data assimilation : a one dimensional study. *Q. J. R. Meteorol. Soc.*, **128**, 1267-1386.

L'Ecuyer, T. S., and G. L. Stephens, 2002: An estimation-based precipitation retrieval algorithm for attenuating radars. *J. Appl. Meteorol.,* **41**, 272-285.

Lhermitte, R., 1990: Attenuation and Scattering of Millimeter Wavelength Radiation by Clouds and Precipitation. *J. Atm. Ocean. Tech.*, **7**, 464-479.

Li, J.-L., and Coauthors, 2012: An observationally based evaluation of cloud ice water in CMIP3 and CMIP5 GCMs and contemporary reanalyses using contemporary satellite data. *J. Geophys. Res*., **117**, D16105, doi:10:1029/2012JD017640.

McNally AP., 2002: A note on the occurrence of cloud in meteorologically sensitive areas and the implications for advanced infrared sounders. *Q. J. R. Meteorol. Soc*., **128**, 2551-2556.

Meneghini, R., and T. Kozu, 1990: *Spaceborne weather radar*. Artech House. 199 pp.

.

Miller, S.D. and G.L.Stephens, G.L.,2001: CloudSat instrument requirements as determined from ECMWF forecasts of global cloudiness. *J. Geophys. Res*., **106**, D16 17,713-17,733.

OSCAR, 2016: A web based resource developed by WMO in support of Earth Observation applications, studies and global coordination. https://www.wmo-sat.info/oscar/

Palerme, C., and Coauthors, 2014: How much snow falls on the Antarctic ice sheet? *The Cryosphere*, **8**, 1577-1587.

Pazmany, A, J., and Coauthors, 1999: Polarization Diversity Pulse-Pair Technique for Millimetre-Wave Doppler Radar Measurements of Severe Storm Features. *J. Atmos. Ocean Technol.*,**16**, 1900–1910, 1999.

Salonen, K., J. Cotton, N. Bormann and M. Forsythe, 2012: Characterizing AMV Height-Assignment Error by Comparing Best-Fit Pressure Statistics from the Met Office and ECMWF Data Assimilation Systems. *J. Appl. Meteor. Climatol.*, **54**, 225-242, doi: 10.1175/JAMC-D-14-0025.1.

Schutgens, N. A., 2008: Simulated Doppler radar observations of inhomogeneous clouds. *J. Atmos. Oceanic Technol.*, 25, 26–42, doi:10.1175/2007JTECHA956.1.

Stephens, G. L., and Coauthors, 2008: CloudSat mission: Performance and early science after the first year of operation. *J. Geophys. Res.,***113**, D009982.

Skolnik, M.I., 1981: *Introduction to radar systems*, McGraw-Hill, 579pp.

Stoffelen, A., and Coauthors, 2005: The atmospheric dynamics mission for global wind measurement. *Bull. Amer. Meteor. Soc.,* **86**, 73-87.

Sy O. O., and Coauthors, 2014: Simulation of EarthCARE Spaceborne Doppler Radar Products using Ground-based and Airborne Data: Effects of Aliasing and Non-Uniform Beam-filling. *IEEE Trans. Geosci. Rem. Sens*, **99**, 1-17, doi: 10.1109/TGRS.2013.2251639.

Tanelli, S., E. Im, S. L.Durden, L. Facheris, D. Giuli, 2002: The Effects of Nonuniform Beam Filling on Vertical Rainfall Velocity Measurements with a Spaceborne Doppler Radar. *J. Atmos. Oceanic Technol.*, **19**, 1019-1034.

Tanelli, S., S.L. Durden, E. Im, K.S. Pak, D. G. Reinke, P. Partain, J.M. Haynes, and R. T. Marchand, 2008: CloudSat's Cloud Profiling Radar After Two Years in Orbit:

Performance, Calibration, and Processing. *IEEE Trans. Geosci. Rem. Sens*, **46**, 3560-3573. 1-17.

Wolde, M., and G. Vali, 2001: Polarimetric signatures from ice crystals observed at 95GHz in winter clouds. Part I: Dependence on crystal form. *J.Atmos. Sci.*, **58**, 828-841.

Zhang, W., 2016: The vision of Space-based component of WMO Integrated Global Observing Systems (WIGOS) in 2040 – Anticipating Requirements and New Space Technologies. 2016 Eumetsat Meteorological Satellite Conference. Darmstadt.

Table 1. The horizontal wind requirements in the lower troposphere for global NWP from OSCAR (2016).

	Uncertainty	Horizontal resolution	Vertical resolution	Observing Cycle
Goal	2 m/s	15km	0.5km	1hr
Breakthrough	3m/s	100km	1km	6hr
Threshold	5m/s	500km	3km	12hr

Table 2. A Possible WIVERN Radar Configuration

Parameter	Value	Units
Operating frequency	94	GHz
Pulse repetition frequency	≈ 4	kHz
Pulse width	3.3	μs
Range resolution	500	m

Antenna diameter	1.8 x 2.9	m
Antenna scan rate	8	rpm
Off-zenith surface angle	41.4	degrees
Orbit height	500	km
Slant range	650	km
Height resolution	800	m
H-V pulse separation	20	μs
Folding velocity	40	m s^{-1}
Doppler accuracy (20km integration, Z> - 20dBZ)	2	m s^{-1}

Table 3.The contribution of the top five observation types to reducing forecast errors for Met Office, ECMWF and MeteoFrance global forecast models. The sixth row are the contributions from scatterometers. HSIR Hyper-spectral infra red; MWSI Microwave sounding/imager; SL Surface/Land; A/C aircraft winds and temp; RS Radio soundings of winds, T and q; GPS-RO – GPS radio occultation.

	Met Office (Oct 2016)	ECMWF (May-Aug 2016)	MeteoFrance (April 2015)
1	HSIR 31.5%	MWSI 36.0%	MWSI 30%
2	MWSI 23.8%	HSIR 30.3%	HSIR 18%
3	AMV 11.9%	A/C 8.4%	A/C 13%
4	SL 8.6%	AMV 6.5%	RS 12%
5	A/C 7.9%	GPS-RO 4.7%	AMV 8%
Scatterometers	3.8 %	5.2%	7%

Table 4. The numbers of raw and assimilated wind observations for ECMWF for u-wind data and their mean assigned error for an arbitrary 12 hour-long window data assimilation cycle starting 00UTC on 2016/10/01.

	TOTAL	AMV	A/C
Raw (pre-QC)	6,527k	3.573.381 54.7%	495,000 7.6%
Assimilated	424k	144.099 34.0%	179,550 42.3%
Fraction assimilated		4.0%	36.3%
Assigned error (m/s)		4.61 m/s	2.27 m/s

FIGURE CAPTIONS

Fig. 1. The WIVERN concept. The dashed black lines correspond to the scanning ground track. For every 7.5 second revolution the satellite advance 50 km. The red arrows are indicative of the wind circulation. The background image (credit: JAXA/NASA/Colorado State Univ., Natalie D. Tourville) corresponds to an overpass of the NASA's CloudSat Satellite over Super Typhoon Atsani on August 19, 2015 at 03:27 UTC.

Fig 2. Daily coverage for a possible WIVERN 500-km orbit with 800-km wide ground track and 651-km slant path. Light green, one visit per day; dark green – two; blue - three.

Fig. 3. Theoretical random error in the line of sight (LOS) retrieved Doppler velocity for WIVERN as a function of target reflectivity for a 20μs H –V pulse separation and a 3.5 m s^{-1} Doppler width due to satellite motion. Single pulse SNR of 0dB for a -19dBZ target. Solid Lines: Red – 1-km integration (10 pulse pairs); Blue – 5 km (50 pulse pairs); Black – 20km (200 pulse pairs) and a Signal to Ghost Ratio (SGR) = ∞. Dashed lines SGR = 0dB. Dotted

lines SGR = -5dB.

Fig. 4. Top row: CloudSat observations of the fraction of the time a cloud is present with a reflectivity exceeding a given threshold as a function of height for an along ground track integration length of 20 km. Left: Tropical clouds. Right: Mid-latitude clouds between 30°N to 60°N. Bottom row: The fraction of the echoes in the top row at each height that have an echo with reflectivity 20dB stronger either 2km above or below that height (see text for details of how this leads to ghosts).

Fig 5. WIVERN surface clutter and viewing geometry a) WIVERN surface clutter for a flat surface with σ_0 =0 dB. Results for a Gaussian antenna with a 3dB-beamwidth of 0.08^0 are also provided as a reference. b) WIVERN viewing geometry, antenna pattern and schematic for understanding NUBF effects.

Fig. 6. Reconstructed WIVERN reflectivity from a stratiform precipitation event observed by CloudSat over Western Pacific between -19°S and -7°S using a 5-km integration length. Left panel: The black dashed line corresponds to the contour where the standard deviation of Doppler velocity is 2 m s^{-1} while the magenta line corresponds to the region where the SCR=20 dB. A T_{hv} =20 µs has been assumed. Right panel: same as the left panel for the WIVERN LDR reconstructed from climatological a-priori LDR. The gray lines here correspond to SGR=3dB while the white line is the rain rate (in mm hr^{-1}) from the CloudSat 2B-RAIN product.

Fig. 7. The fraction of WIVERN profiles, integrated along-track for 5 km, where winds at a given height can be derived with an accuracy of 2 m s^{-1} for various T_{hv} values, derived from

CloudSat profiles with an assumed LDR value and recent observations of surface clutter returns over the ocean (blue) and over land (red), excluding mountains and cities. Note the effect of ghost returns from the surface affecting the retrieval at heights dependent upon T_{hv}.

Fig. 8. Figure 8. Observations at Chilbolton, UK at 45° elevation showing the increased random error in the velocity estimates due to ghosts on 27 June 2017. A) The signal to noise ratio (SNR) in the H channel, B) The signal to ghost ratio (SGR) in the H channel due to the depolarisation of the V channel shifted by 3km in range, C) 'PP20' The velocity derived from the H-V (20μs/3km) pulse pairs with a folding velocity of 40 m s^{-1}, D) Upper trace: the 'true' velocity' (red line) derived from a pulse separation of 160μs at a height of 4.54 km and the PP20 velocity from the H-V pulses (black). Note the increased noise in the black trace when SGR and SNR are low. Lower trace: the observed rms error obtained by comparing the 'true' PP160 velocity with the PP20 'H-V' velocity (black), and the close agreement with the theoretical errors from the SNR and SGR (red), and from the H-V correlation (green). The high wind shear case accompanied by large vertical reflectivity gradients observed on 28 Aug 2017 is displayed in panels E and F. For details see the text.

Fig. 9. Statistics of the AMV winds assimilated into the Met Office global model from Meteosat-10 for the month of December 2016. Left: The mean assigned observation error of U (m/s) as a function of pressure and latitude. Right: the number of winds assimilated as a function of pressure. The maximum numbers are found at around 900 hPa over the Southern Oceans, followed by heights of 200-400 hPa at all latitudes. Note the relatively low number of winds from mid-levels.

Fig. 10. Comparison of the number of assimilated AMV winds in the ECMWF model and the predicted number of WIVERN winds. Left: The number of assimilated AMV (U-wind) observation counts for 20161001 LWDA cycle (12 hour window) per 10^6 km^2 (1000 by 1000 km box). Data are thinned to one observation per 200 by 200 km box per height level. Right: As for ECMWF but the predicted number for WIVERN simulated using CloudSat data with Z>-17dBZ for 5km along track integration, scaled appropriately for WIVERN sensitivity and increased swath. One observation is counted for each 80 by 80 km box.

Sidebar 1.

WHY POLARIZATION DIVERSITY?

The simple answer is that at 94GHz we need to have two pulses that are very close together because the motion of the satellite combined with the finite beamwidth of the radar results in a rapid decorrelation of the phases of the return signals. If the pulses are close together they will both be in the cloud at the same time: to distinguish them, WIVERN transmits pairs of pulses with alternating polarization -H (red) and V (blue) spaced by a short time separation, T_{hv} and receive the return signals in both polarizations (panel A). Because of the orthogonality of the polarisations, the horizontally and vertically polarized pulses are transmitted, backscattered and propagate through the atmosphere independently so that the returns from the two closely spaced pulses can be separated. Cross-polar interferences are typically weak and WIVERN signal processing includes ways for removing their effects.

In panel C the red H pulse is at height ‘h’, and at a short time later (e.g. T_{hv} =20 μs), the blue V pulse has moved (e.g. 3 km) along the slant path and is at height ‘h’ (panel D). The estimation of the Doppler velocity is based on the phase change between the backscattered signals of these two pulses. Panel B (green shaded region) shows that for a T_{hv} of only 20 µs the targets have not had time to reshuffle, so the phases remain correlated and can be measured accurately. The maximum unambiguous phase shift value of ±180° is reached when the cloud particle targets move one quarter of a wavelength (800µm at W-band), equivalent, with T_{hv}=20 µs, to a folding velocity of ±40 m s^{-1} (top x-axis in panel B).

Contrast this with the situation encountered in conventional pulse pair (panel E) when the phase change is derived between two pulses with the same polarization, with the second red ‘H’ pulse trailing 130µs (≈ 20km) behind the first so that only one pulse at a time is in the troposphere. Because of the fast movement of the satellite, the targets will appear to have almost completely reshuffled (red shaded region in panel B), the phase difference will be very noisy, and the maximum ‘folding’ velocity only about 6 m s^{-1}, far below that required for retrieving line-of-sight winds.

Sidebar 2.

GHOST ECHOES

The formation of ghosts is illustrated in a bounce diagram for the profile indicated by the black arrow in Fig. 6. The cross-polar (V-) component of the transmitted H-pulse reflected at the point S_1 on the surface interferes with the rain co-polar signal of the second (V-) pulse transmitted after T_{hv} = 20 µs and scattered along the line A_1B_1 in time–distance space. In the same manner, the trailing edge of the pulse reflected in the cross-channel at the point S_2 adds up to the rain signal along the line A_2B_2.At the V-receiver the co-polar V-signals backscattered by rain in the grey-shaded rhombus $A_1A_2B_2B_1$ region are overcome by the ground clutter cross-polar return of the first pulse (blue shaded regions). These ghost signals appear in the second pulse centred around an altitude of $cT_{hv}\cos(\theta_{inc})/2$, (2.25 km for this T_{hv}). Because the ground clutter is uncorrelated with the rain signals this only worsens the Doppler velocity estimates according to the SGR (Fig. 3). The same phenomenon can occur when strong vertical reflectivity gradients are present concurrently with strongly depolarizing targets (e.g. red shaded region).

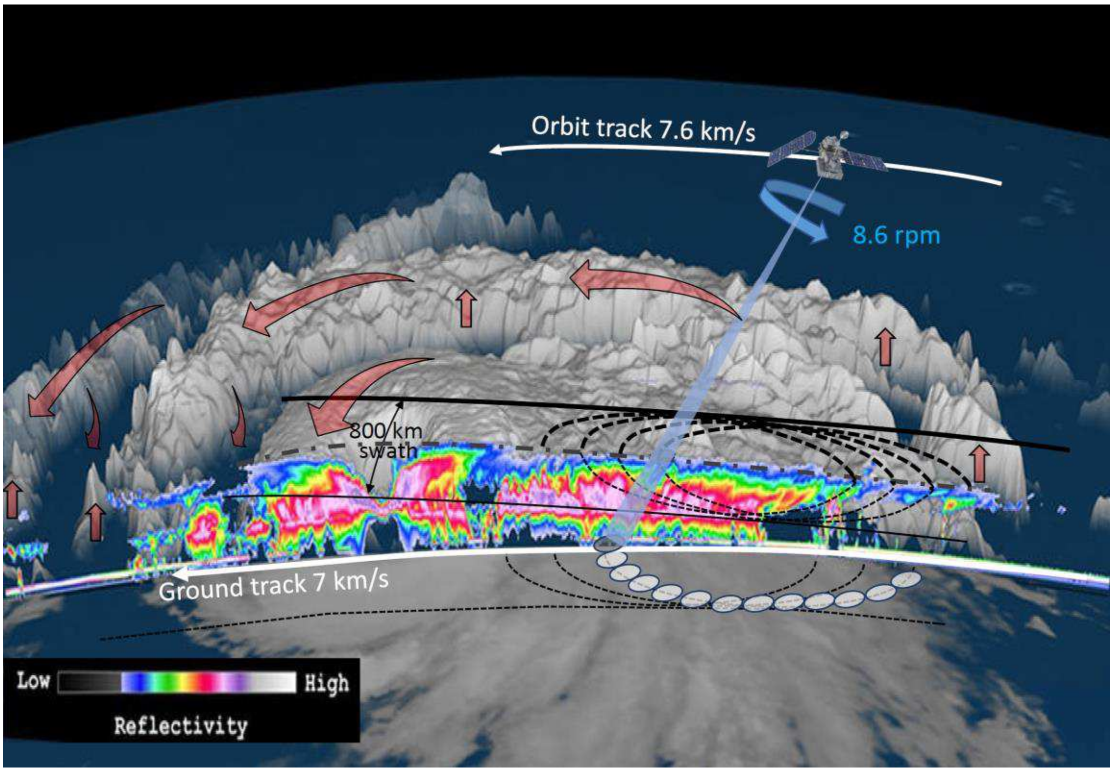

Figure 1. The Wivern concept. The dashed black lines correspond to the scanning ground track. For every 7 second revolution the satellite advance 50 km. The red arrows are indicative of the wind circulation. The background image (credit: JAXA/NASA/Colorado State Univ., Natalie D. Tourville) corresponds to an overpass of the NASA's CloudSat Satellite over Super Typhoon Atsani on August 19, 2015 at 03:27 UTC.

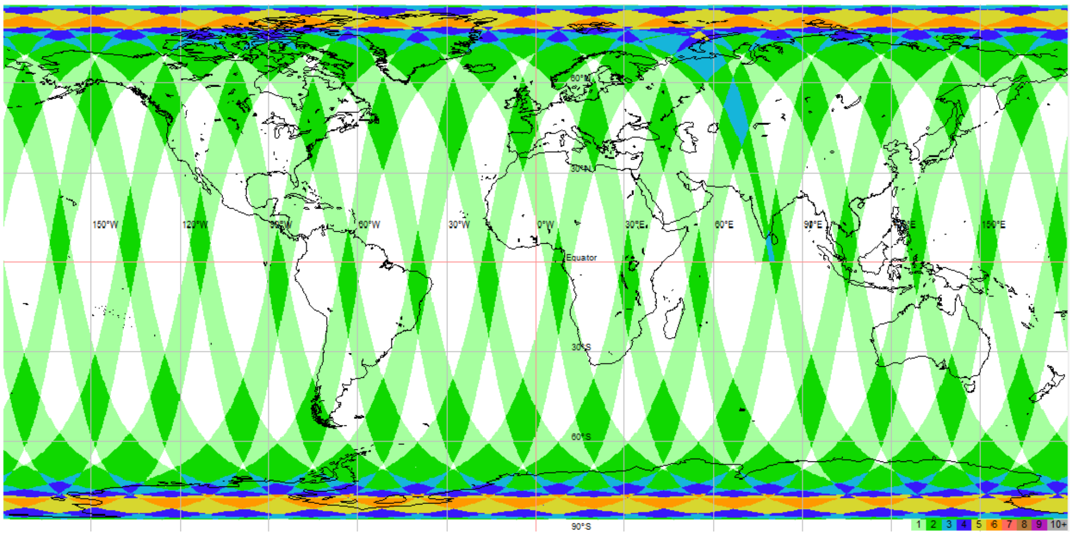

Figure 2. Daily coverage for a possible WIVERN 500-km orbit with 800-km wide ground track and 651-km slant path. Light green, one visit per day; dark green – two; blue - three.

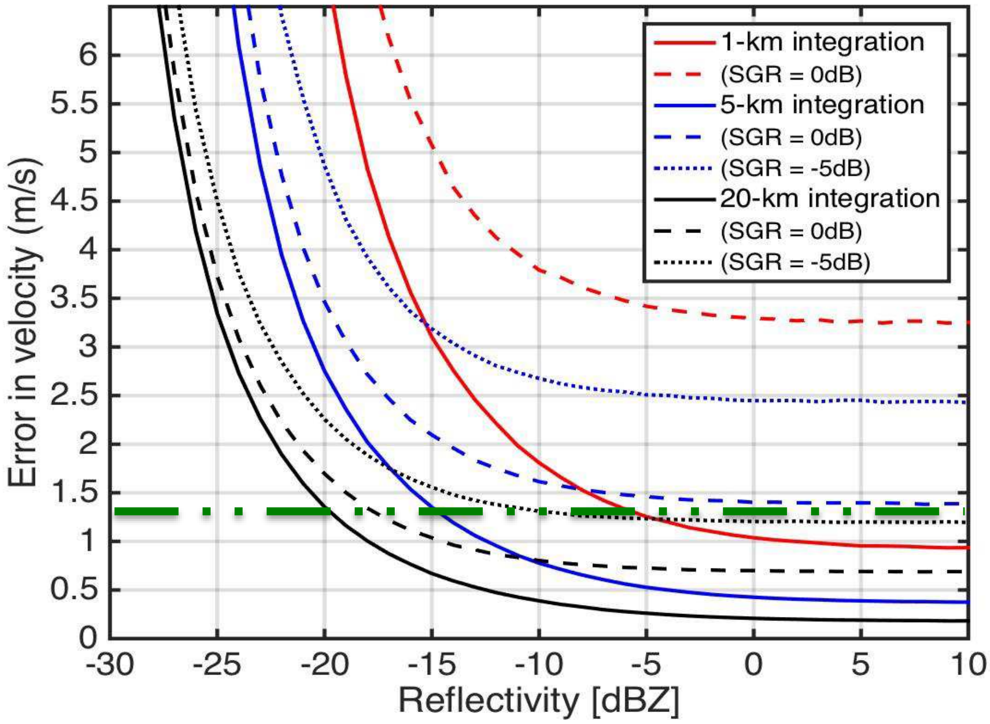

\

Figure 3. Theoretical random error in the line of sight (LOS) retrieved Doppler velocity for WIVERN as a function of target reflectivity for a 20µs H –V pulse separation and a 3.5 m s^{-1} Doppler width due to satellite motion and a single pulse SNR of 0dB for a -19dBZ target. Solid Lines: Red – 1-km integration (10 pulse pairs); Blue – 5 km (50 pulse pairs); Black –

20km (200 pulse pairs) and a Signal to Ghost Ratio (SGR) = ∞. Dashed lines SGR = 0dB. Dotted lines SGR = -5dB

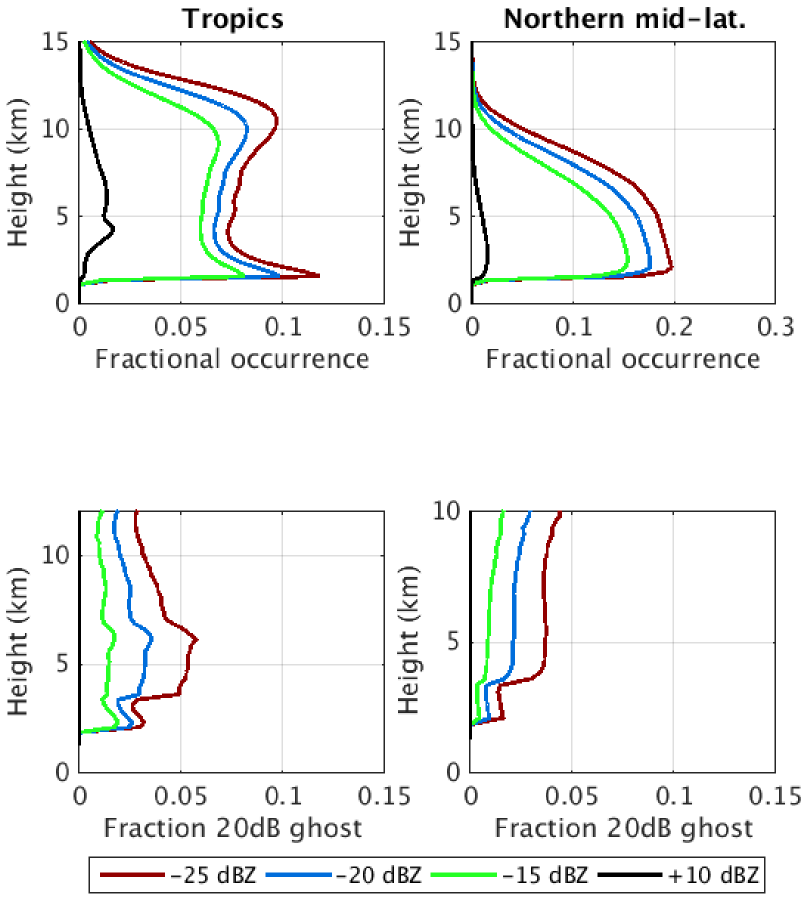

Figure 4. Top row: CloudSat observations of the fraction of the time a cloud is present with a reflectivity exceeding a given threshold as a function of height for an along ground track integration length of 20 km. Left: tropical clouds. Right: mid-latitude clouds between 30°N to 60°N. Bottom row: the fraction of the echoes in the top row at each height that have an echo with reflectivity 20dB stronger either 2km above or below that height (see text for details of how this leads to ghosts).

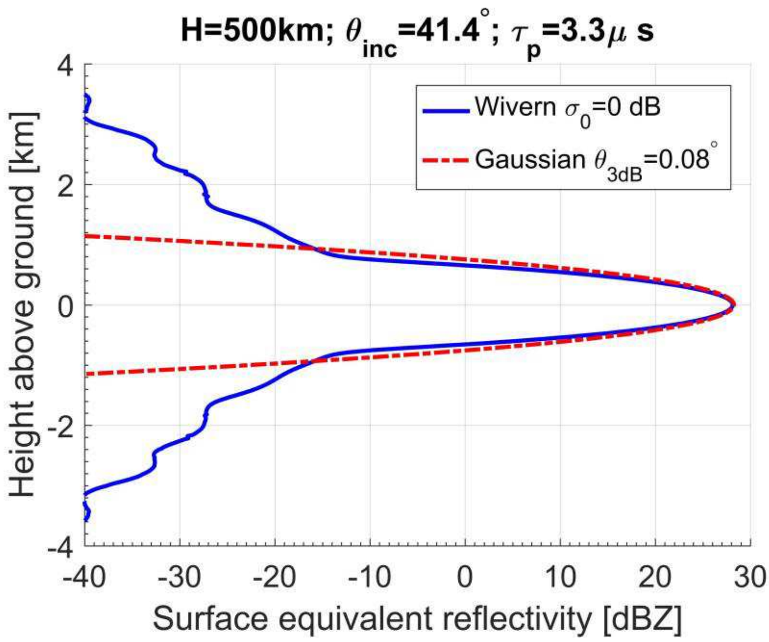

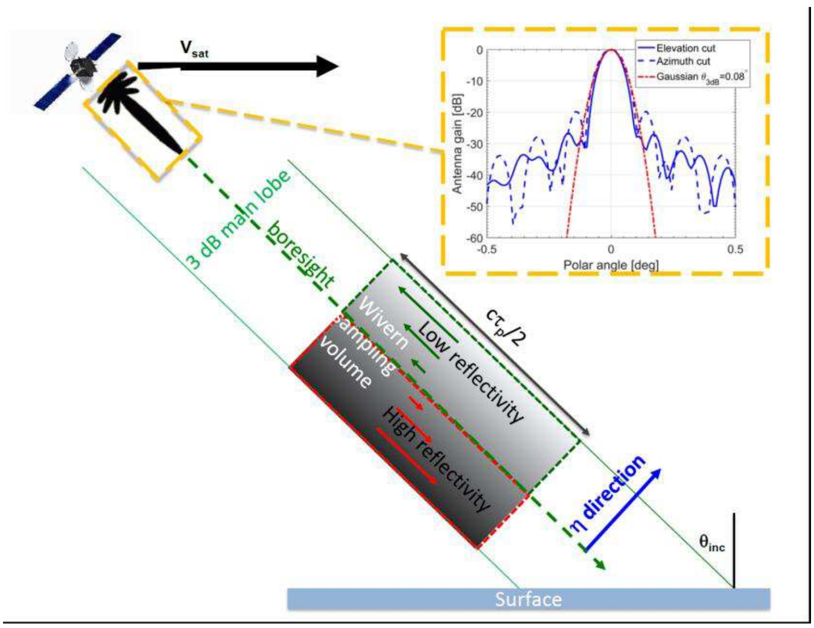

Figure 5: WIVERN surface clutter and viewing geometry

a) WIVERN surface clutter for a flat surface with σ_o =0 dB. Results for a Gaussian antenna with a 3dB-beamwidth of 0.08^0 are also provided as a reference. b) WIVERN viewing geometry, antenna pattern and schematic for understanding NUBF effects.

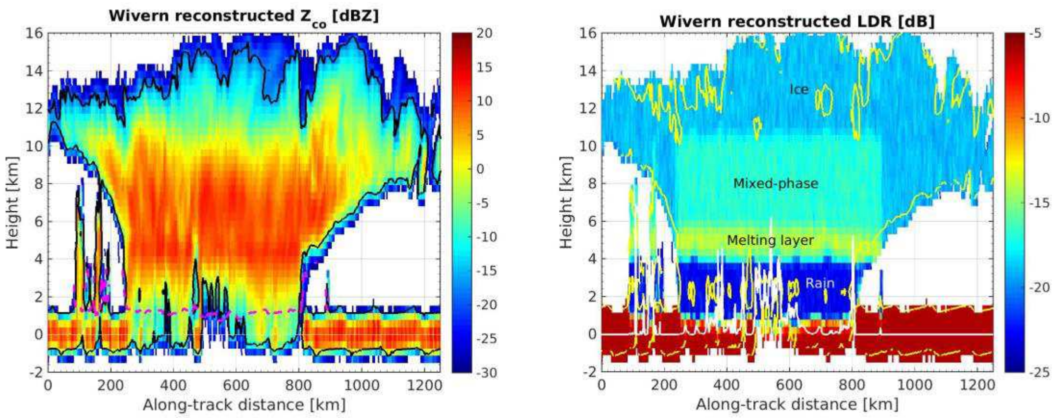

Figure 6. Reconstructed WIVERN reflectivity from a stratiform precipitation event observed by CloudSat over Western Pacific between -19^{o}S and -7^{o}S using a 5-km integration length. Left panel: The black dashed line corresponds to the contour where the standard deviation of Doppler velocity is 2 m s^{-1} while the magenta line corresponds to the region where the SCR=20 dB. A T_{hv} =20 μs has been assumed. Right panel: same as the left panel for the WIVERN LDR reconstructed from climatological a-priori LDR. The gray lines here correspond to SGR=3dB while the white line is the rain rate (in mm hr^{-1}) from the CloudSat 2B-RAIN product.

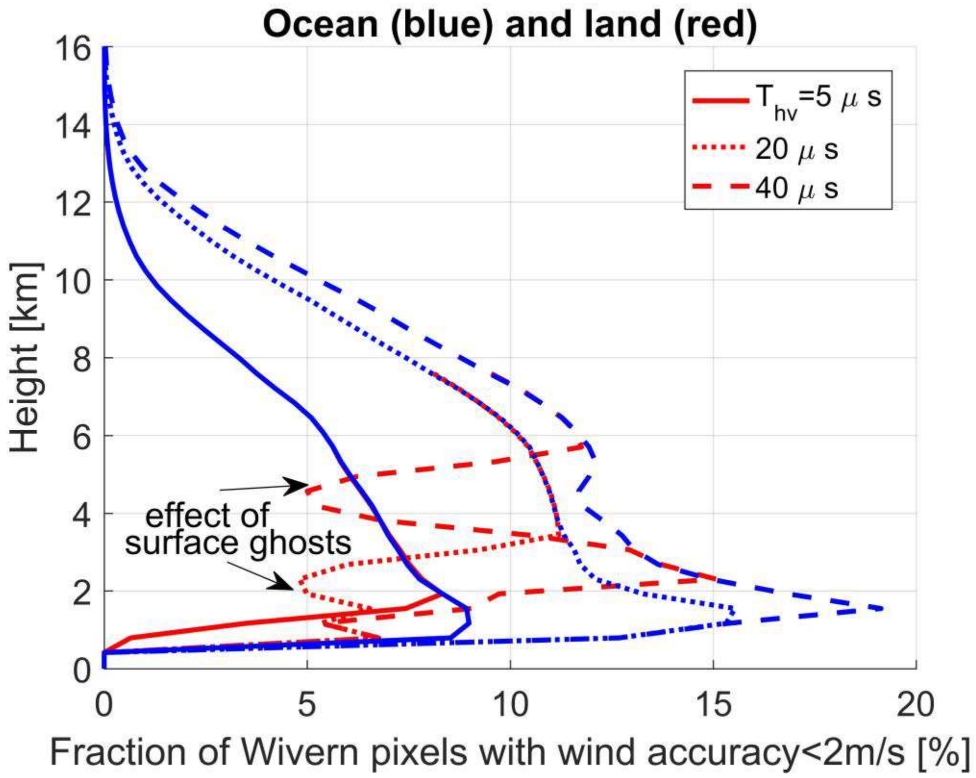

Figure 7. The fraction of WIVERN profiles, integrated along-track for 5 km, where winds at a given height can be derived with an accuracy of 2 m s^{-1} for various T_{hv} values, derived from CloudSat profiles with an assumed LDR value and recent observations of surface clutter returns over the ocean (blue) and over land (red), excluding mountains and cities. Note the effect of ghost returns from the surface affecting the retrieval at heights dependent upon T_{hv}.

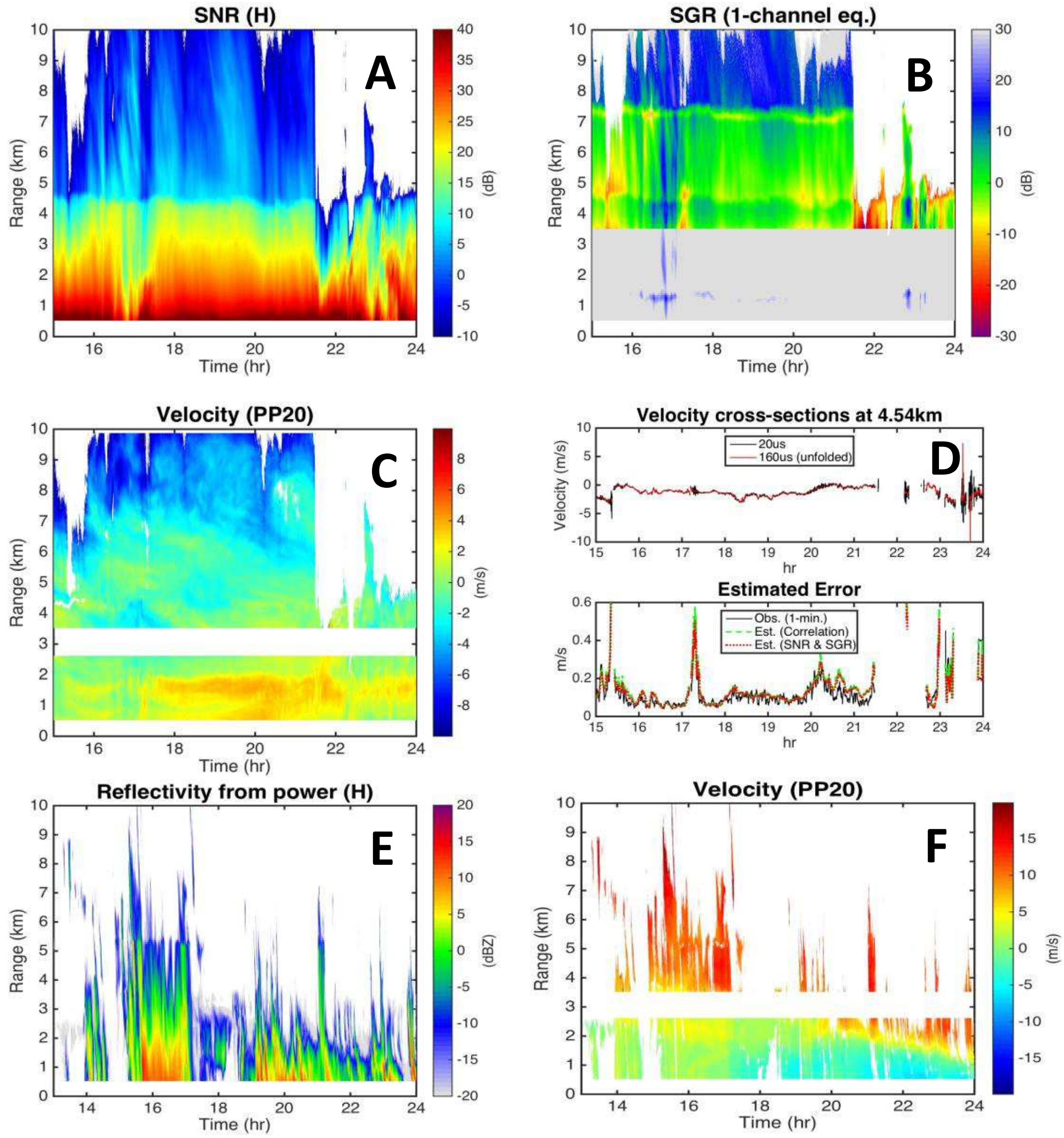

Figure 8. Observations at Chilbolton, UK at 45° elevation showing the increased random error in the velocity estimates due to ghosts on 27 June 2017. A) The signal to noise ratio (SNR) in the H channel, B) The signal to ghost ratio (SGR) in the H channel due to the depolarisation of the V channel shifted by 3km in range, C) 'PP20' The velocity derived from the H-V (20µs/3km) pulse pairs with a folding velocity of 40 m s^{-1}, D) Upper trace: the 'true' velocity' (red line) derived from a pulse separation of 160µs at a height of 4.54 km and the PP20 velocity from the H-V pulses (black). Note the increased noise in the black trace when SGR and SNR are low. Lower trace: the observed rms error obtained by comparing the

'true' PP160 velocity with the PP20 'H-V' velocity (black), and the close agreement with the theoretical errors from the SNR and SGR (red), and from the H-V correlation (green). The high wind shear case accompanied by large vertical reflectivity gradients observed on 28 Aug 2017 is displayed in panels E and F. For details see the text.

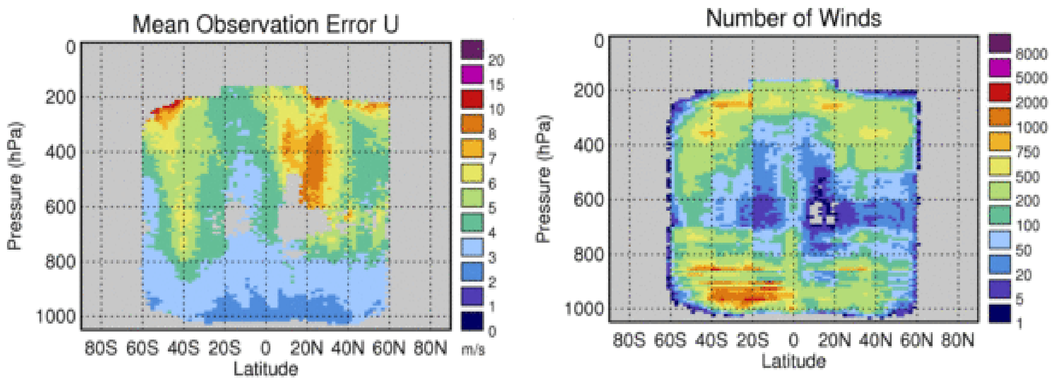

Figure 9. Statistics of the AMV winds assimilated into the Met Office global model from Meteosat-10 for the month of December 2016. Left: The mean assigned observation error of U (m/s) as a function of pressure and latitude. Right: the number of winds assimilated as a function of pressure. The maximum numbers are found at around 900 hPa over the Southern Oceans, followed by heights of 200-400 hPa at all latitudes. Note the relatively low number

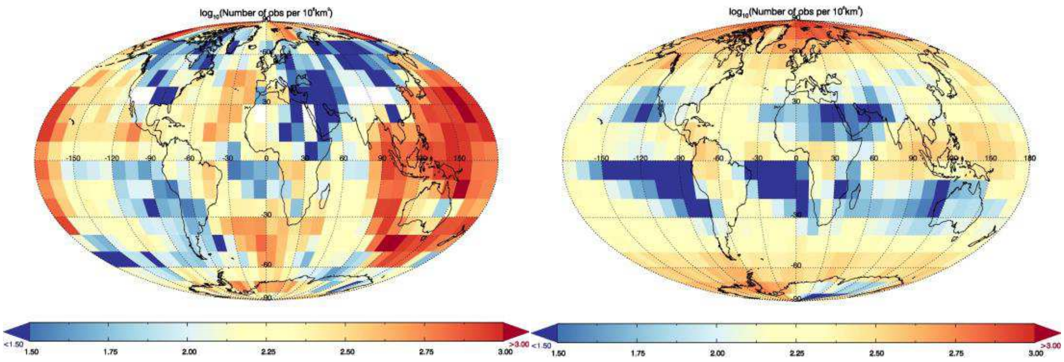

Figure 10. Comparison of the number of assimilated AMV winds in the ECMWF model and the predicted number of WIVERN winds. Left: The number of assimilated AMV (U-wind) observation counts for 20161001 LWDA cycle (12 hour window) per 10^6 km^2 (1000 by 1000 km box). Data are thinned to one observation per 200 by 200 km box per height level. Right: As for ECMWF but the predicted number for WIVERN simulated using CloudSat data with Z>-17dBZ for 5km along track integration, scaled appropriately for WIVERN sensitivity and increased swath. One observation is counted for each 80 by 80 km box.

SIDEBAR ONE: WHY POLARIZATION DIVERSITY?

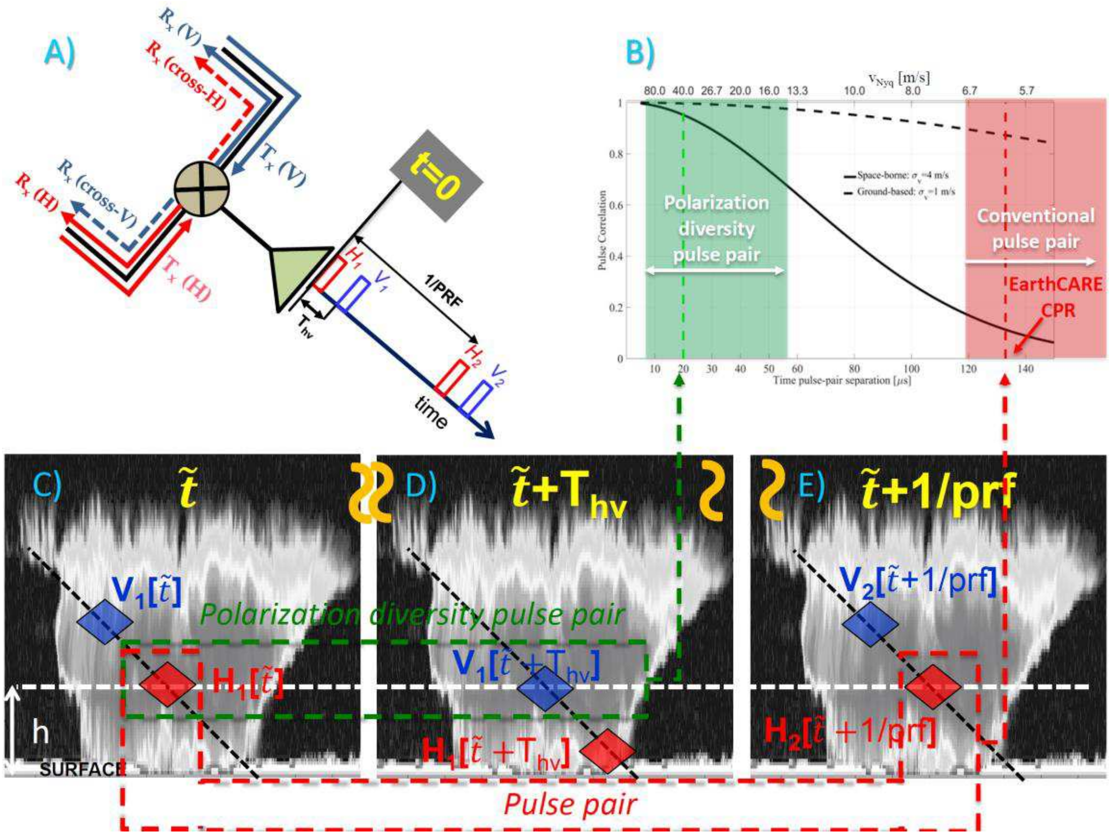

SIDEBAR TWO: GHOST ECHOES